Focal Spot Deconvolution using Deep Convolutional Neural Networks

Jan Kuntz, Joscha Maier,
Marc Kachelrieß, and Stefan Sawall

German Cancer Research Center (DKFZ)
Heidelberg, Germany
www.dkfz.de/ct

Aim

Fast and accurate deconvolution of x-ray projection images blurred by source and detector blur.

Increasing scintillator thickness results in higher efficiency but lower spatial resolution

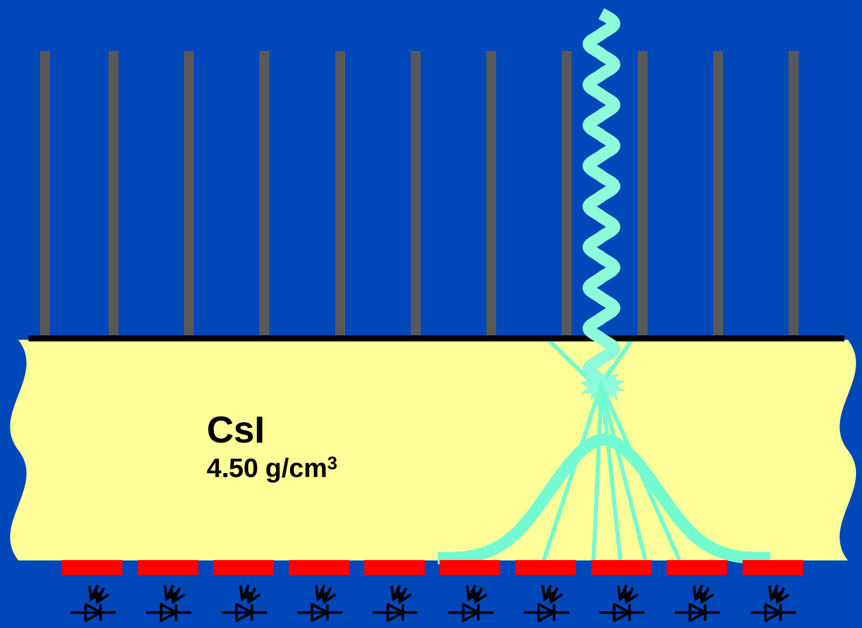

Increasing x-ray power results in shorter scans but extended focal spot size

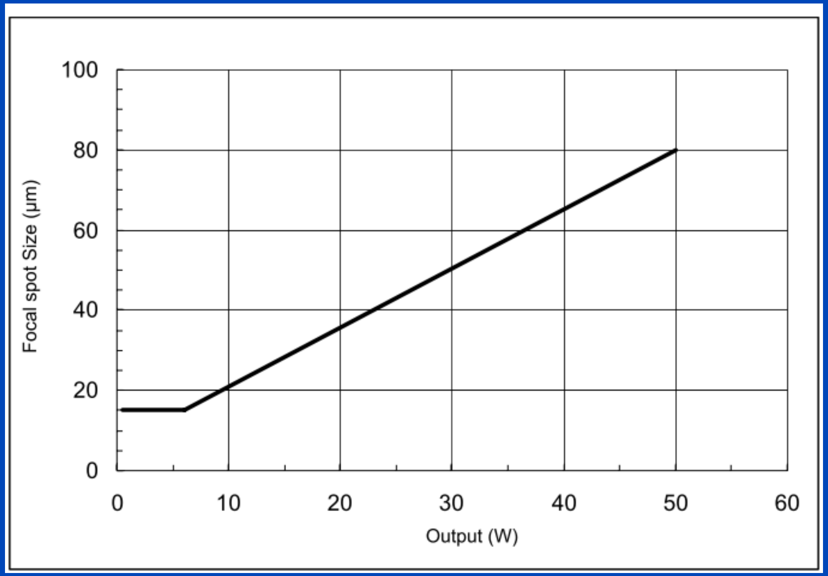

Hamamatsu L10951 Micro-Focus X-ray Source

Detector and Source Blur Models

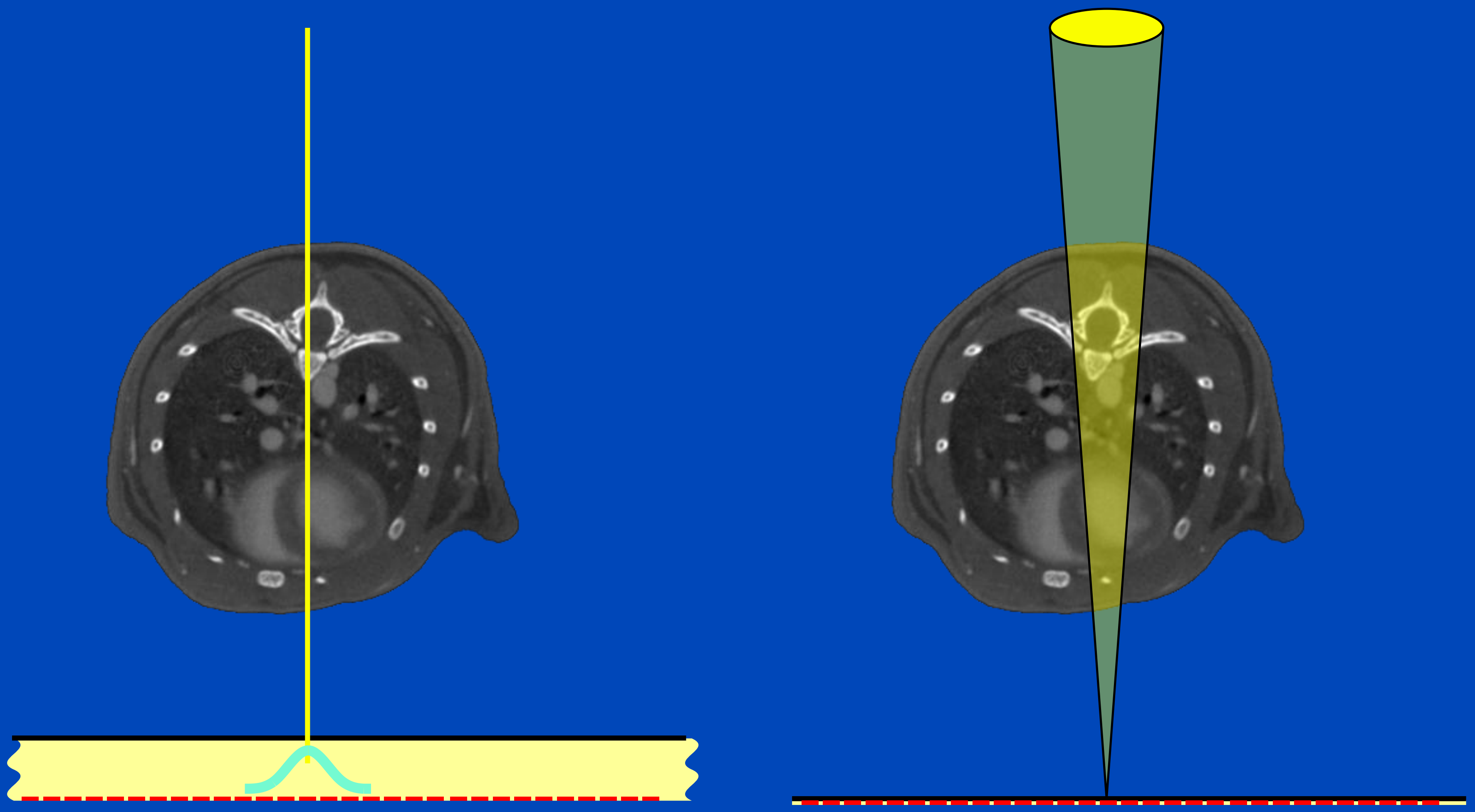

Detector and Source Blur Models

Detector deblurring

- **Image blur caused by the detector can be modeled by a convolution of the ideal projection image with a Gaussian function**

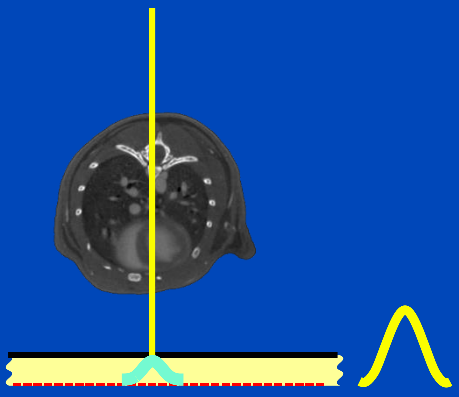

Source deblurring

- **Image blur caused by the focal spot size is depth dependent and can neither be modeled nor corrected with a single Gaussian convolution model**

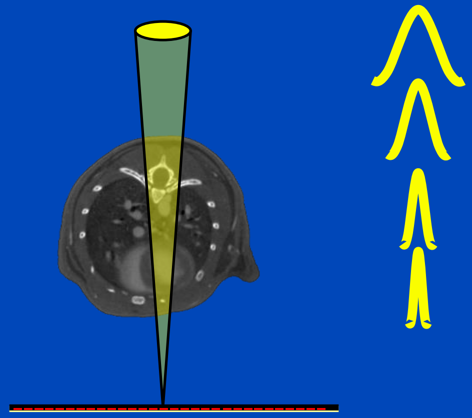

CNN Task

- The aim of CNN deblurring is the restoration of the ideal image information.
- As the ideal image usually is unavailable, a high resolution acquisition can be used as reference

Ideal or HighRes Image

Acquired Image (LowRes)

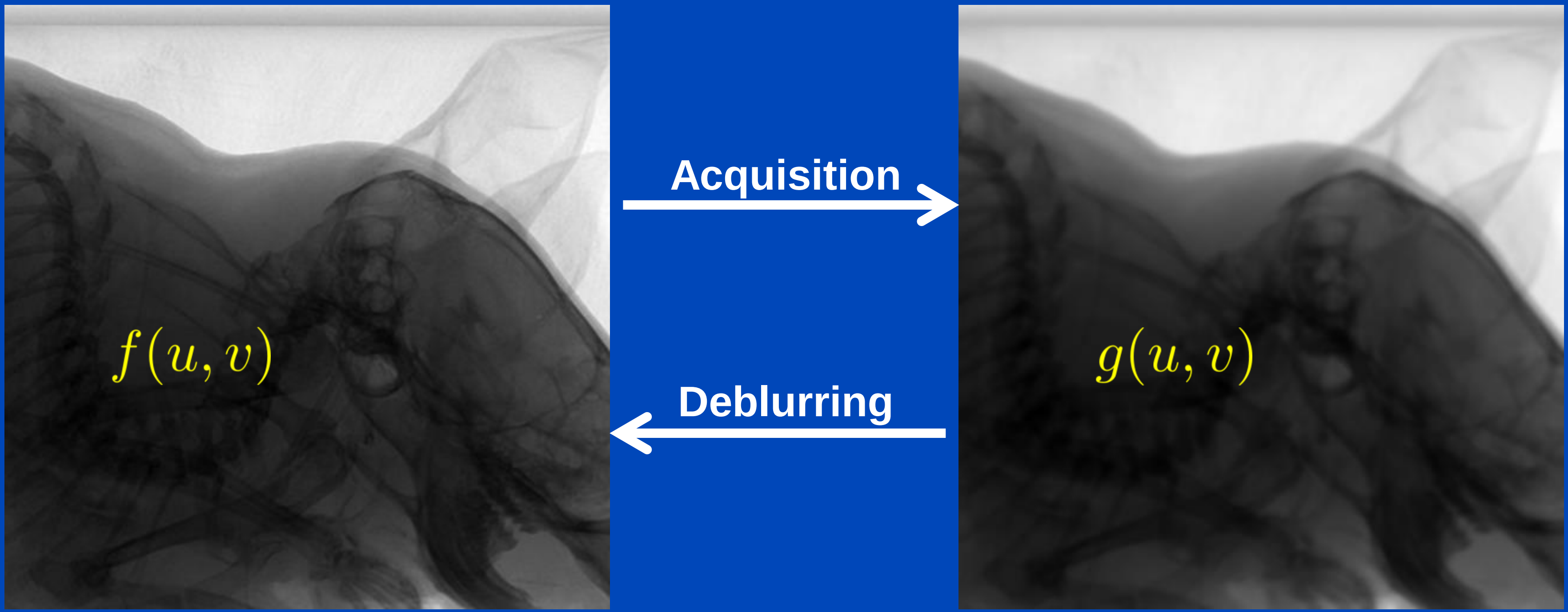

CNN Training and Application

- Modified U-net[1]
- Blurred images were used as input images for the CNN
- High resolution images were used as reference
- Training and application of the CNN was performed in intensity domain
- The CNN was trained for 100 epochs using the Adam optimizer
- Images not included in the training dataset were used for testing

[1]Ronneberger, Fischer, and Brox: "U-net: Convolutional networks for biomedical image segmentation," MICCAI 9351, pp. 234–241, 2015.

U-Net[1] Trained for Deconvolution

Input: Low resolution image
Output: High resolution deblurred image

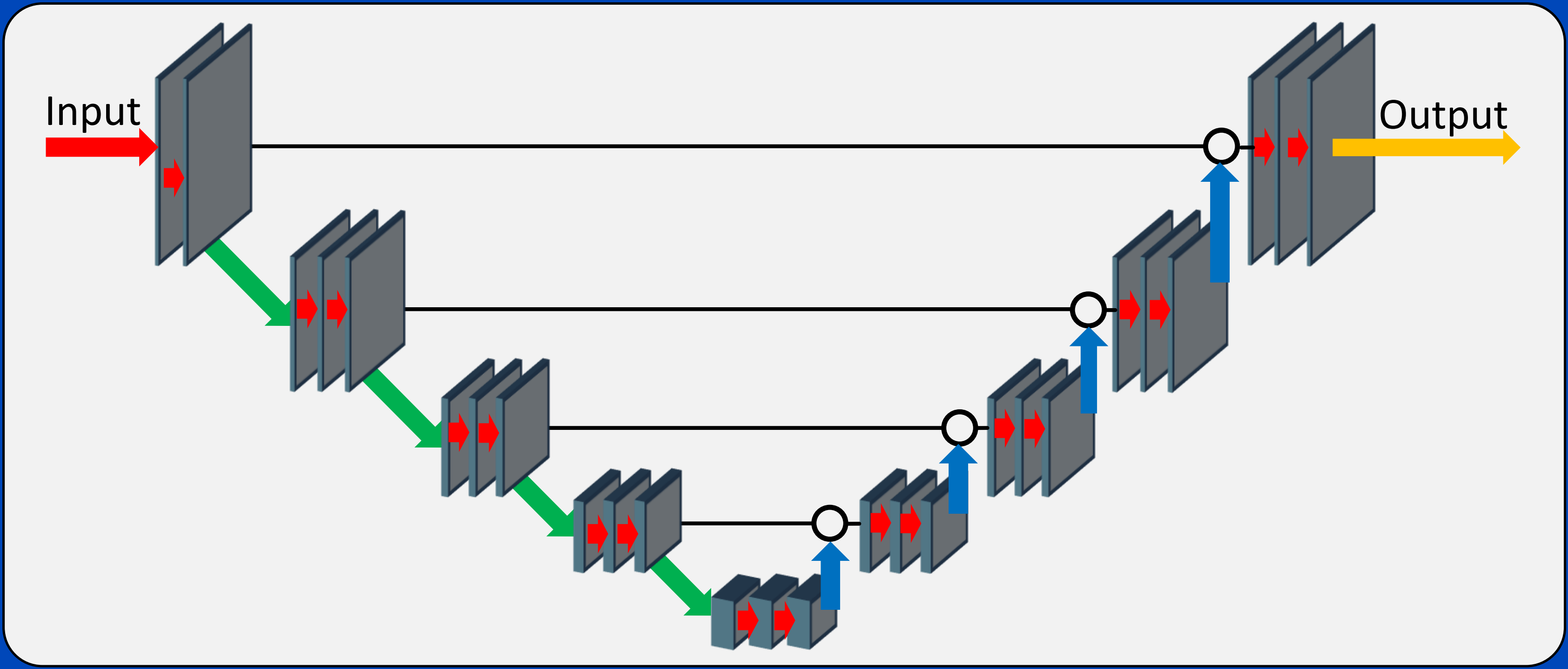

- 3 × 3 Convolution, ReLU
- 3 × 3 Convolution (stride = 2)
- Depth Concatenate
- 3 × 3 Transposed Convolution (stride = 2)

[1]Ronneberger, Fischer, and Brox: "U-net: Convolutional networks for biomedical image segmentation," MICCAI 9351, pp. 234–241, 2015.

Reference: RL Deconvolution

- **Richardson-Lucy deconvolution**
- **Iterative deconvolution using a known point spread function**

$$f_j^{(t+1)} = f_j^{(t)} \sum_i \frac{g_i}{\sum_j k_{ij} f_j^{(t)}} k_{ij}$$

$$\begin{aligned} k_{ij} &= \text{point spread function} \\ f_j &= \text{estimated signal} \\ g_i &= \text{observed signal} \end{aligned}$$

Richardson, W. H. (1972). "Bayesian-Based Iterative Method of Image Restoration". JOSA. 62 (1): 55–59.
Lucy, L. B. (1974). "An iterative technique for the rectification of observed distributions". Astronomical Journal. 79 (6): 745–754.

Experiments

1. High resolution images blurred with a shift invariant Gaussian filter
2. High resolution images blurred with a shift variant filter
3. High and low resolution projection images, measured on a table top system
4. Forward projections of high resolution micro-CT scans

Shift Invariant Blurring

- Single convolution with a Gaussian kernel was used to generate a large number of blurred images from initial high resolution images
- Representing a detector blur model
- Training dataset of 1925 high resolution projections

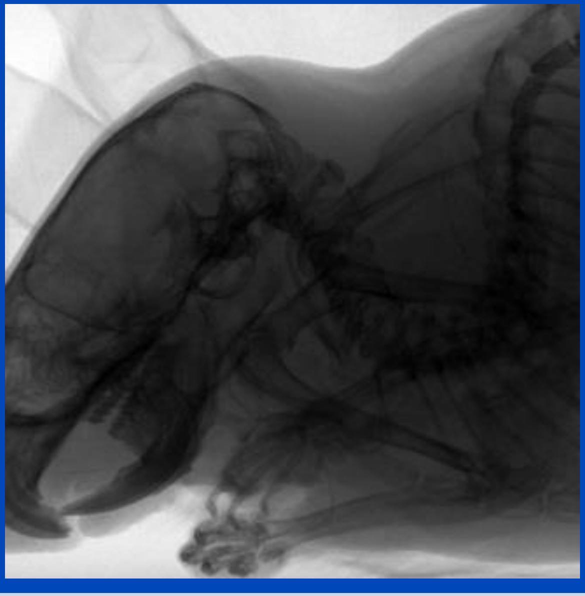

*

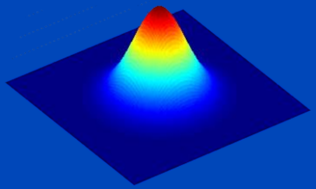

σ = 2 pixel
FWHM = 4.7 pixel

=

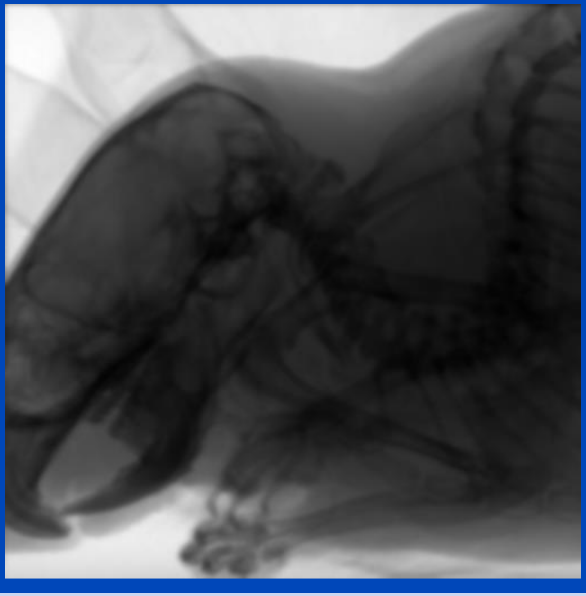

Shift Invariant Blurring

- Comparison of CNN to Richardson-Lucy deconvolution
- $\sigma = 2$ pixel

Original Image | Blurred Image | RL Deblurring | CNN Deblurring

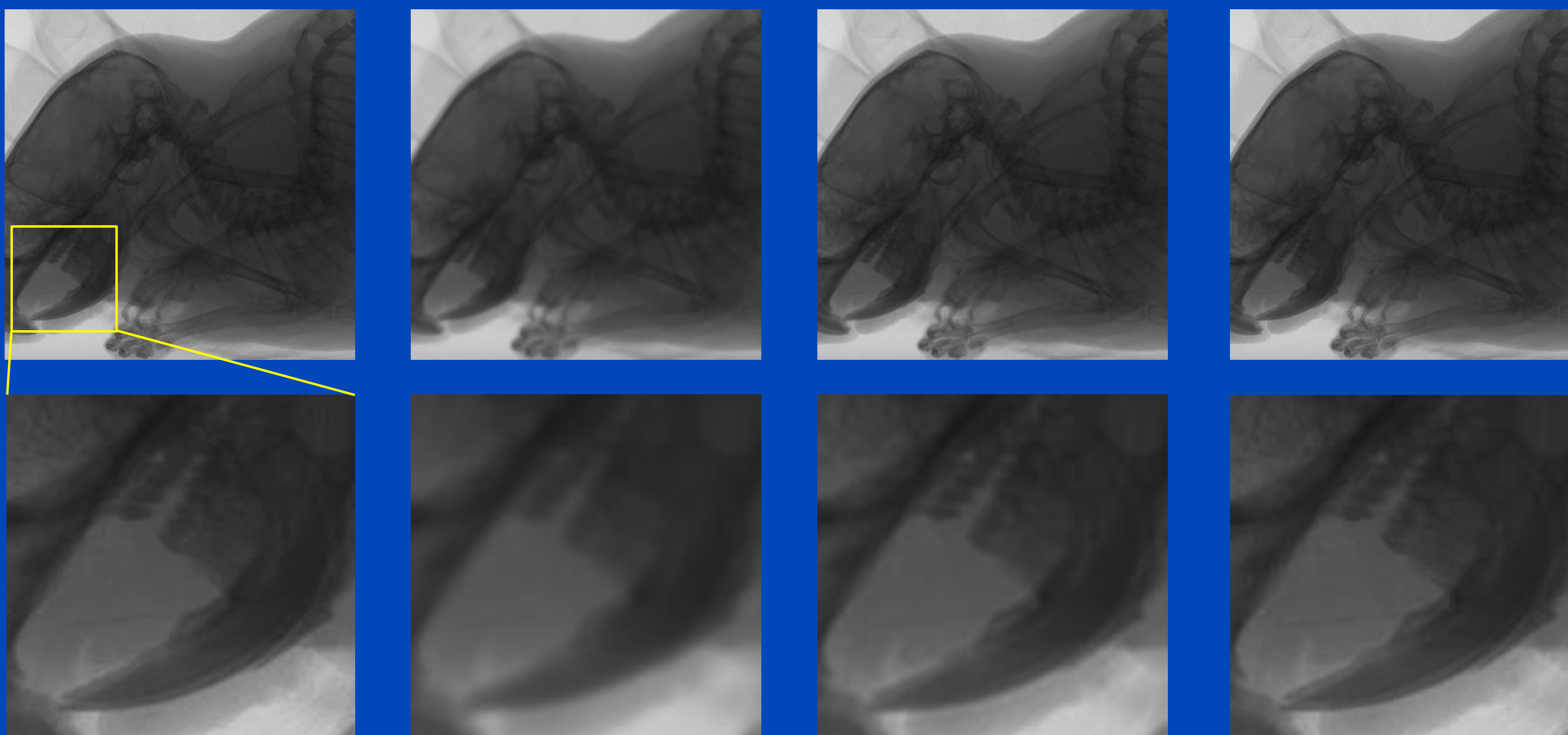

Shift Invariant Blurring

- Comparison of CNN to Richardson-Lucy deconvolution
- $\sigma = 2$ pixel

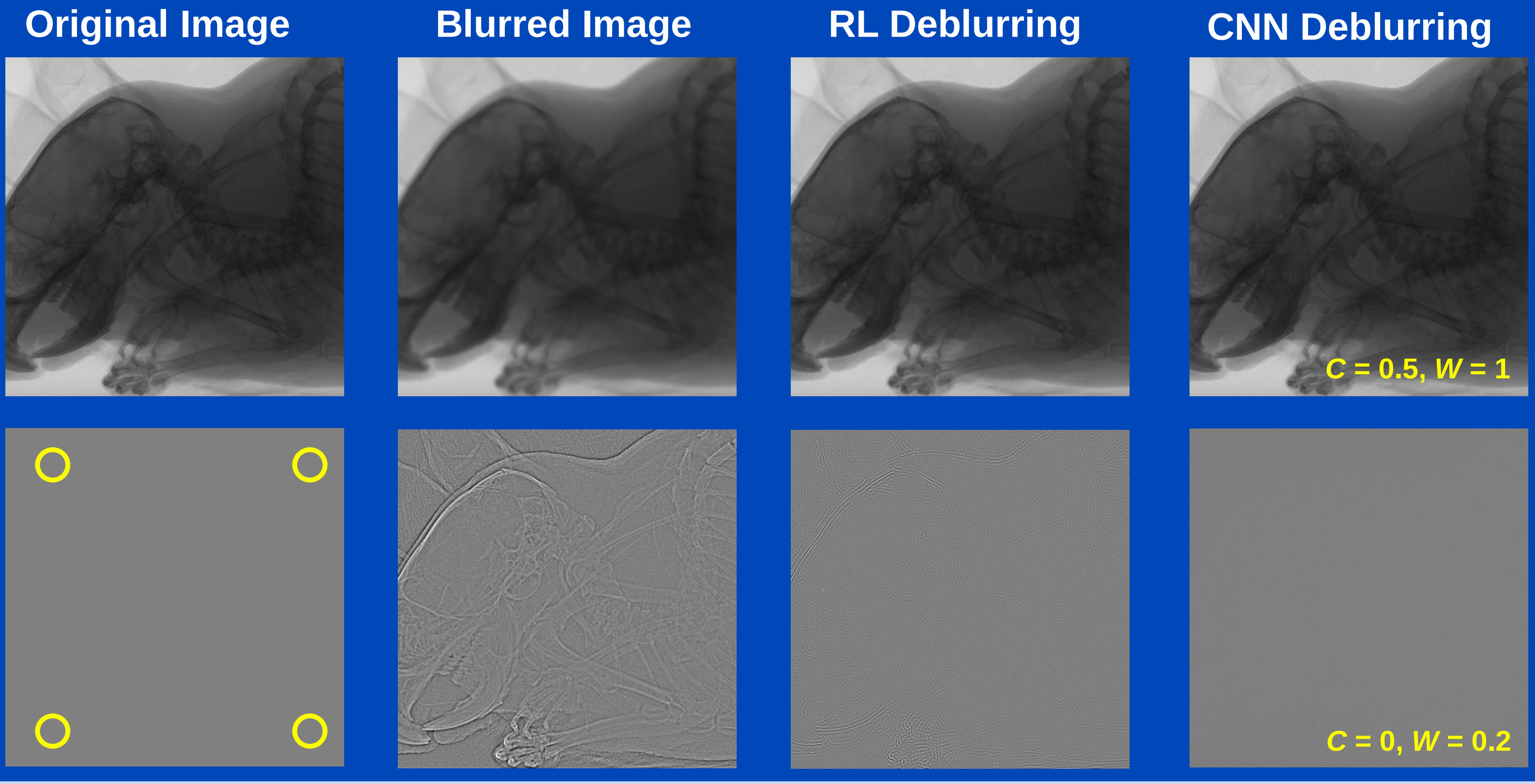

Shift Variant Blurring

- A more general blur model was implemented with a **shift variant** Gaussian
- Gaussian kernel varied from $\sigma = 1$ to $\sigma = 3$ in both directions independently

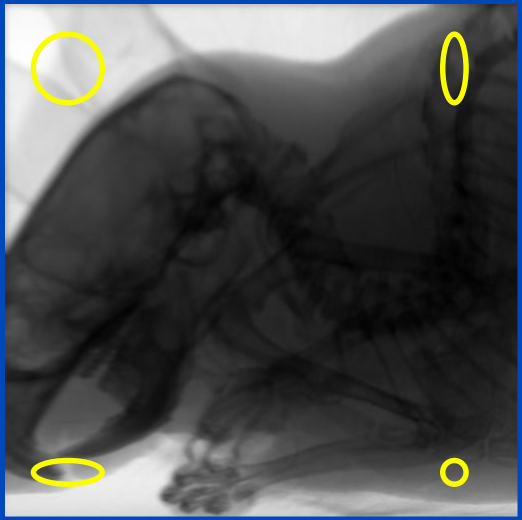

Ellipses indicate 10 × FWHM of filter kernel

Shift Variant Blurring

- Comparison of CNN to Richardson-Lucy deconvolution
- $1 \leq \sigma \leq 3$

Original Image | Blurred Image | RL Deblurring | CNN Deblurring

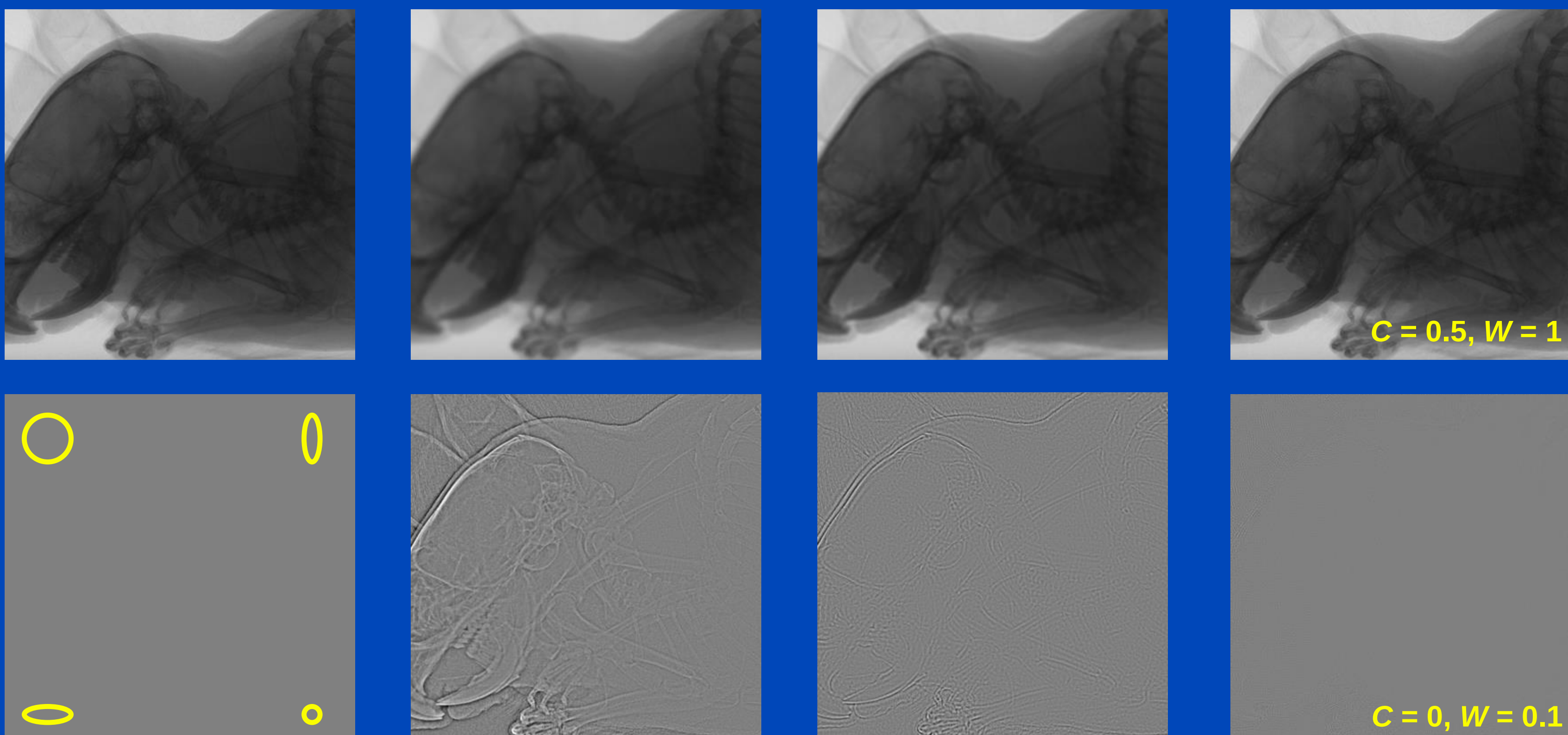

Shift Variant Blurring Including Simulated Noise

- To evaluate the noise characteristics of the deblurring techniques, noise was added to the original image corresponding to 10.000 photons per ray
- Blurring as well as deblurring was performed on noisy projection images using a shift variant kernel
- Variance images of 100 projections representing identical projection geometry were calculated

Shift Variant Blurring Including Simulated Noise

- Noisy images, simulated with 10.000 photons per ray
- $1 \leq \sigma \leq 3$, var images calculated from 100 realizations

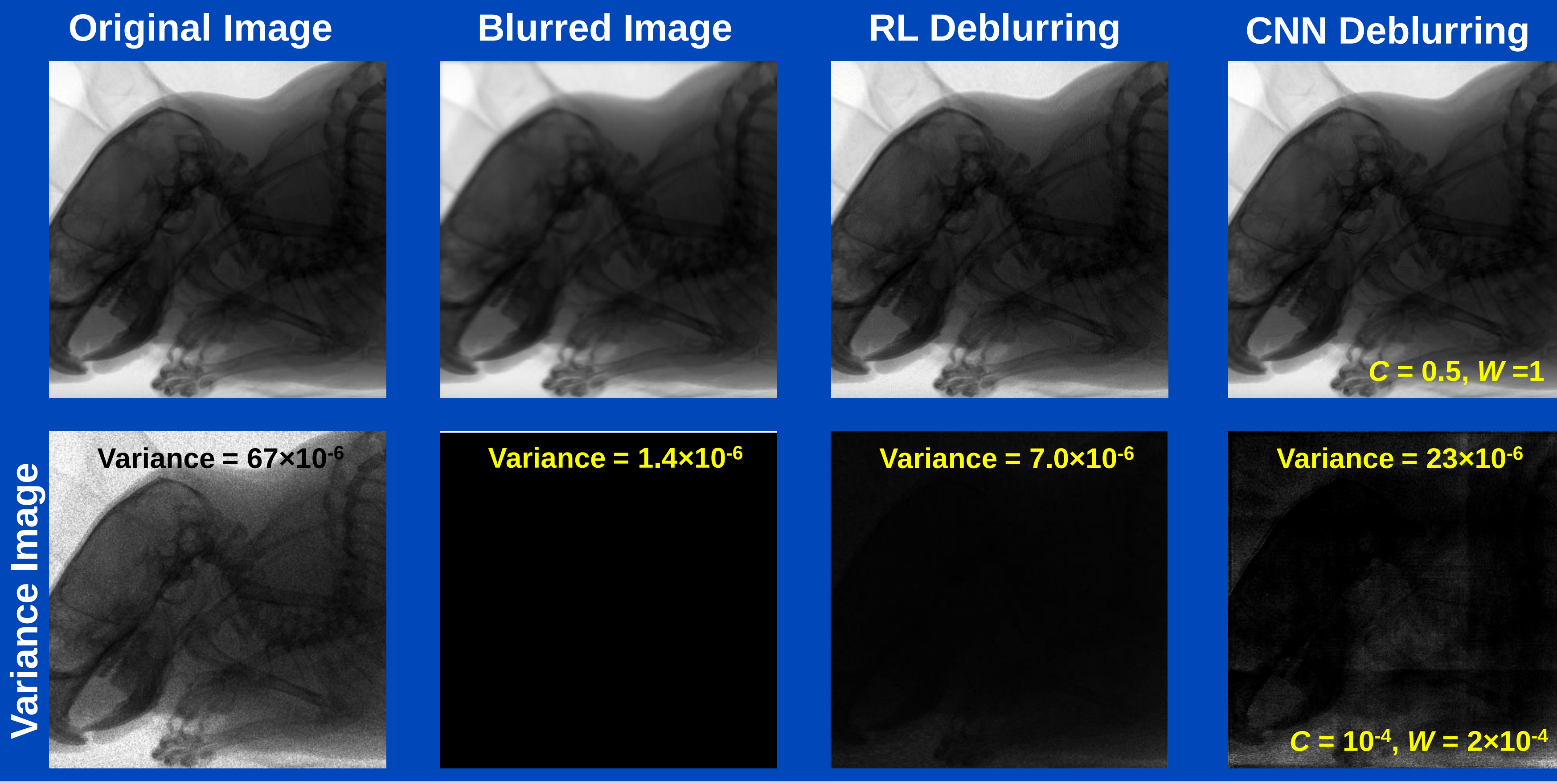

Deconvolution with or of Pictures?

Training data: Cows, Horses, Pigs

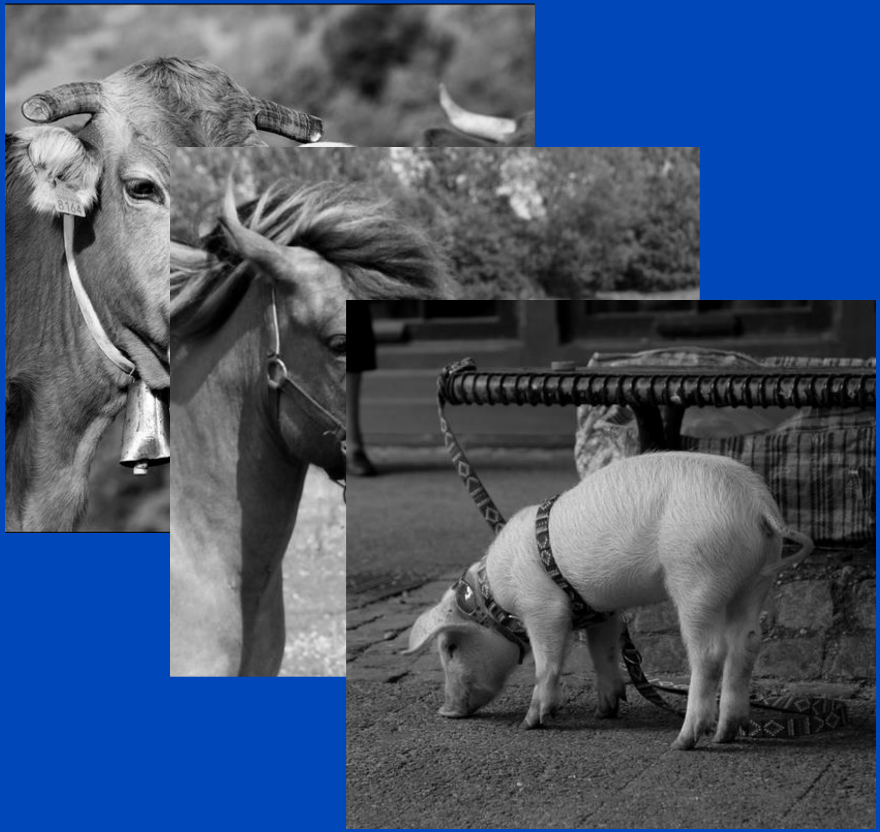

Testing Data: Squirrels

Deconvolution with or of Pictures?

- CNN deconvolution of shift variant and invariant blurred images can be trained and applied to projection images as well as photographs
- Examples from the "*animals with attributes 2"* dataset

Y. Xian, C. H. Lampert, B. Schiele, Z. Akata. "Zero-Shot Learning - A Comprehensive Evaluation of the Good, the Bad and the Ugly", IEEE Transactions on Pattern Analysis and Machine Intelligence (T-PAMI) 40(8), 2018.

Deconvolution with or of Pictures?

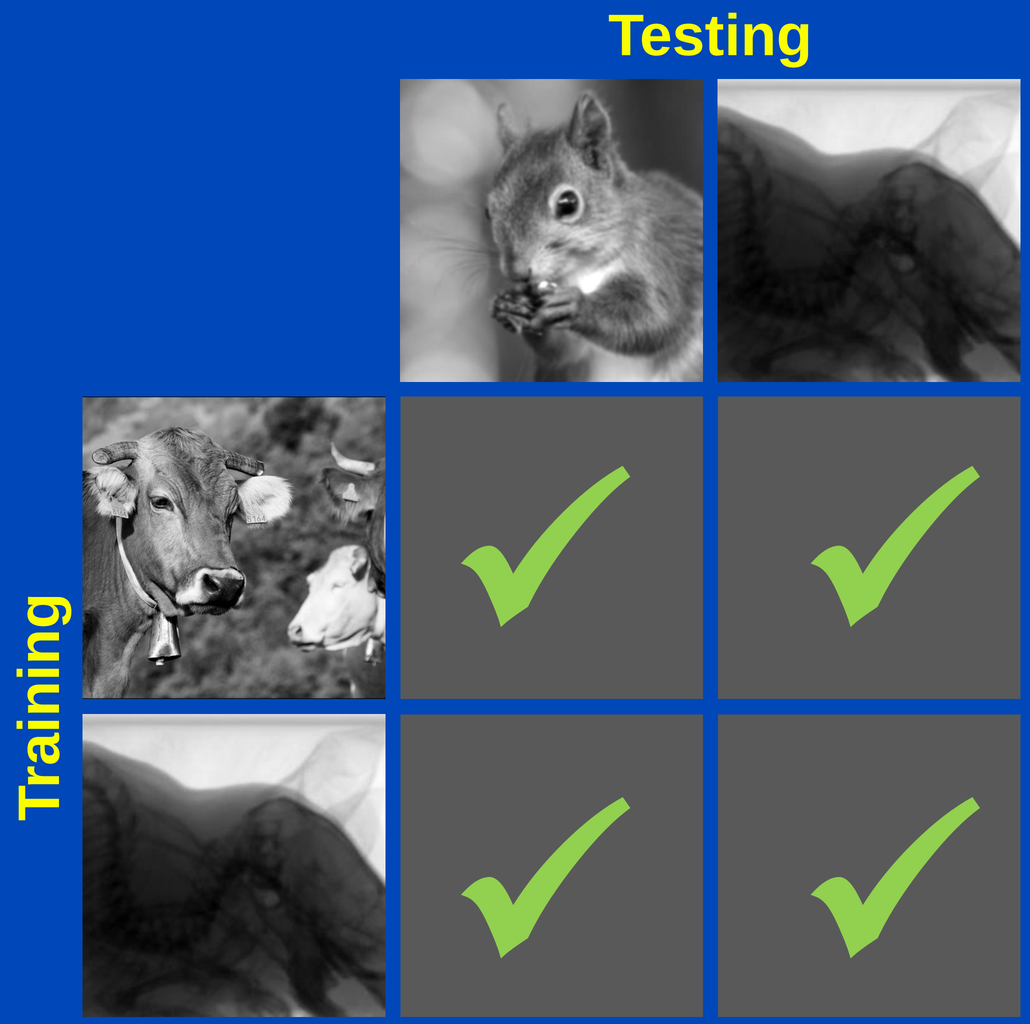

Measurements

- Measurements were performed on a table top CT system
- Two series of projections were acquired for various samples
- Small focal spot: 15 µm (4.8 W)
- Large focal spot: 80 µm (48 W)

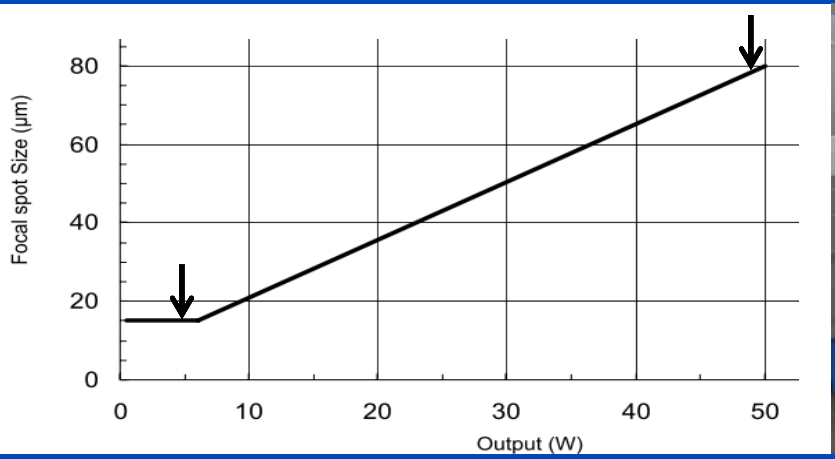

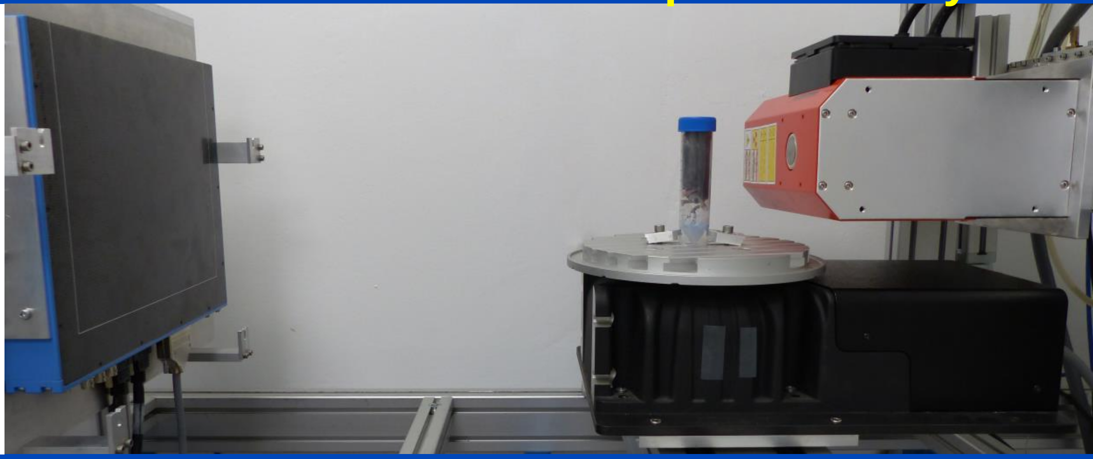

Training on Measured Data

- CNN was trained on 1095 projections of a mouse
- CNN was applied to a head dataset of another mouse

Training

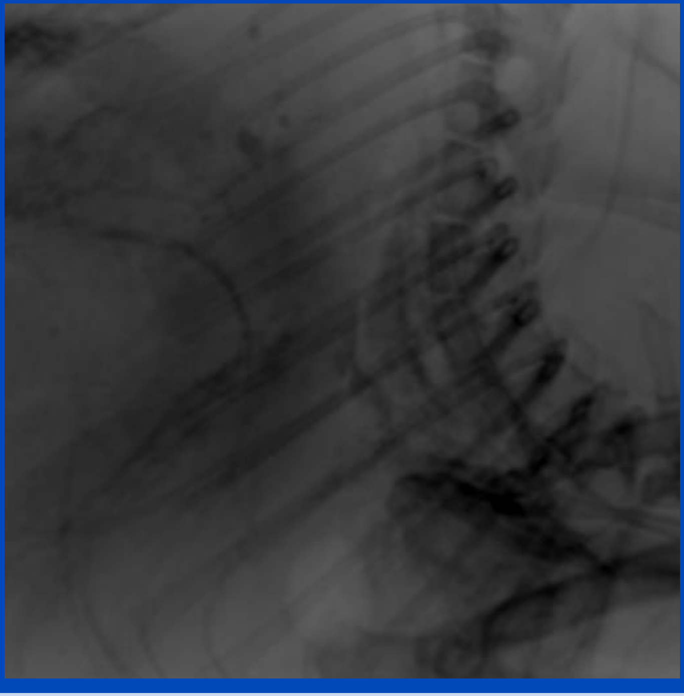

Testing

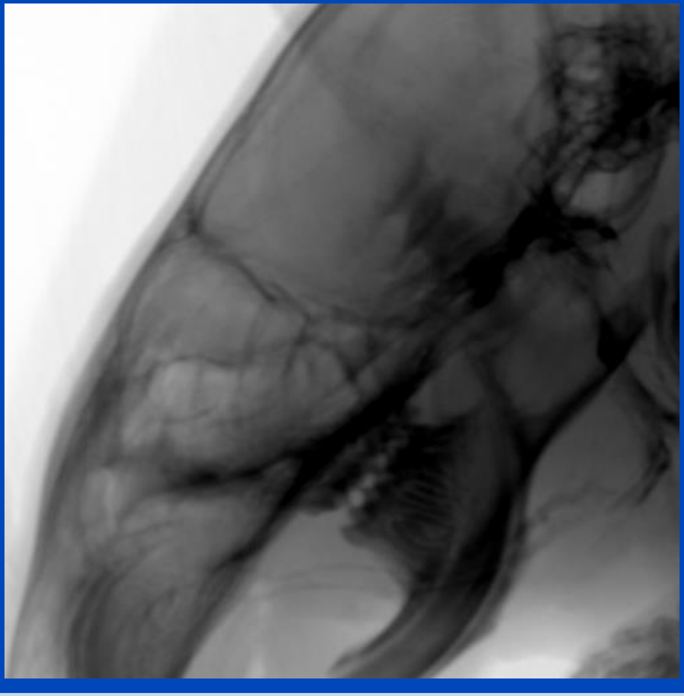

CNN Deblurring with Measured Data

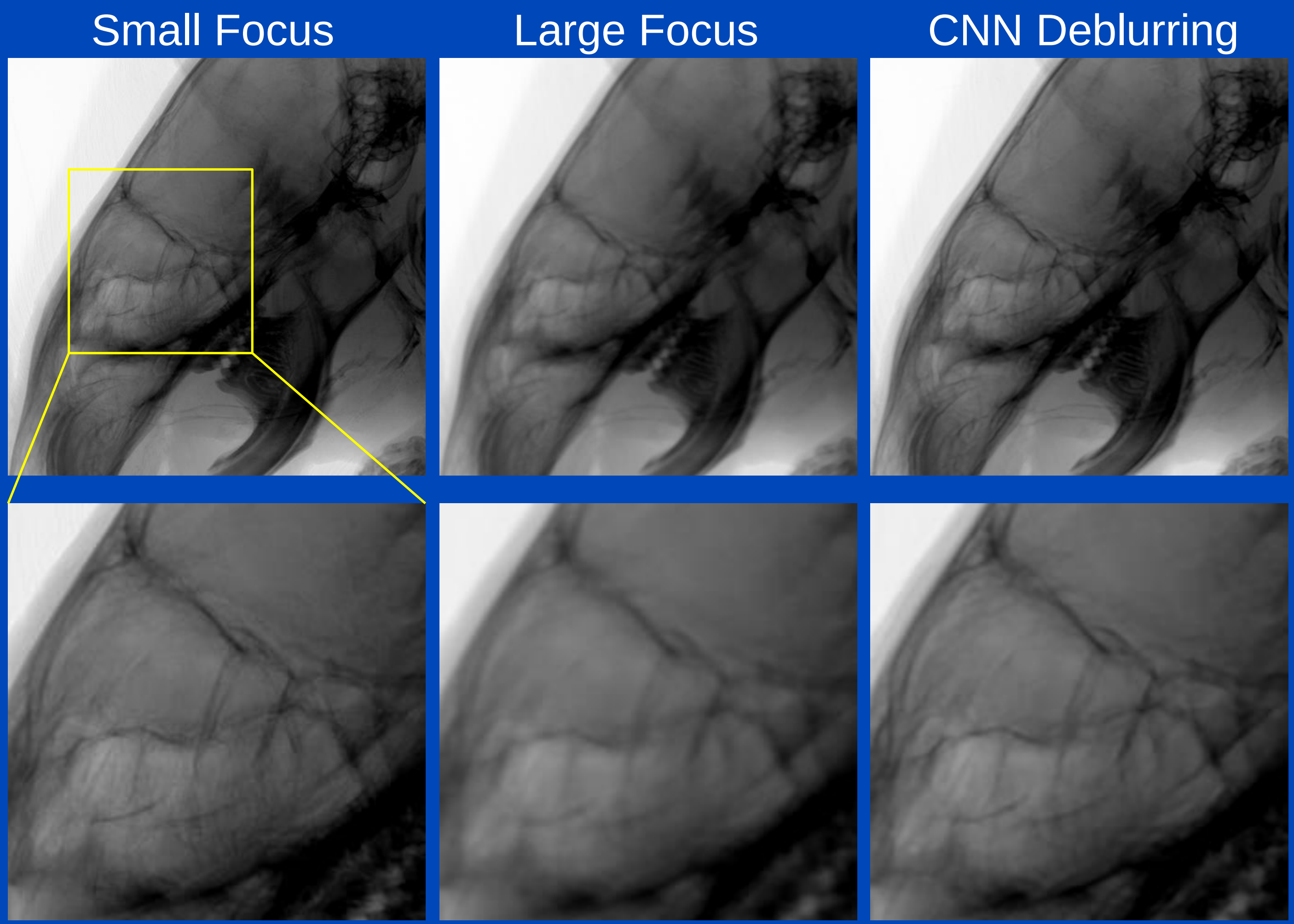

CNN Deblurring with Measured Data

Small Focus | Large Focus | CNN Deblurring

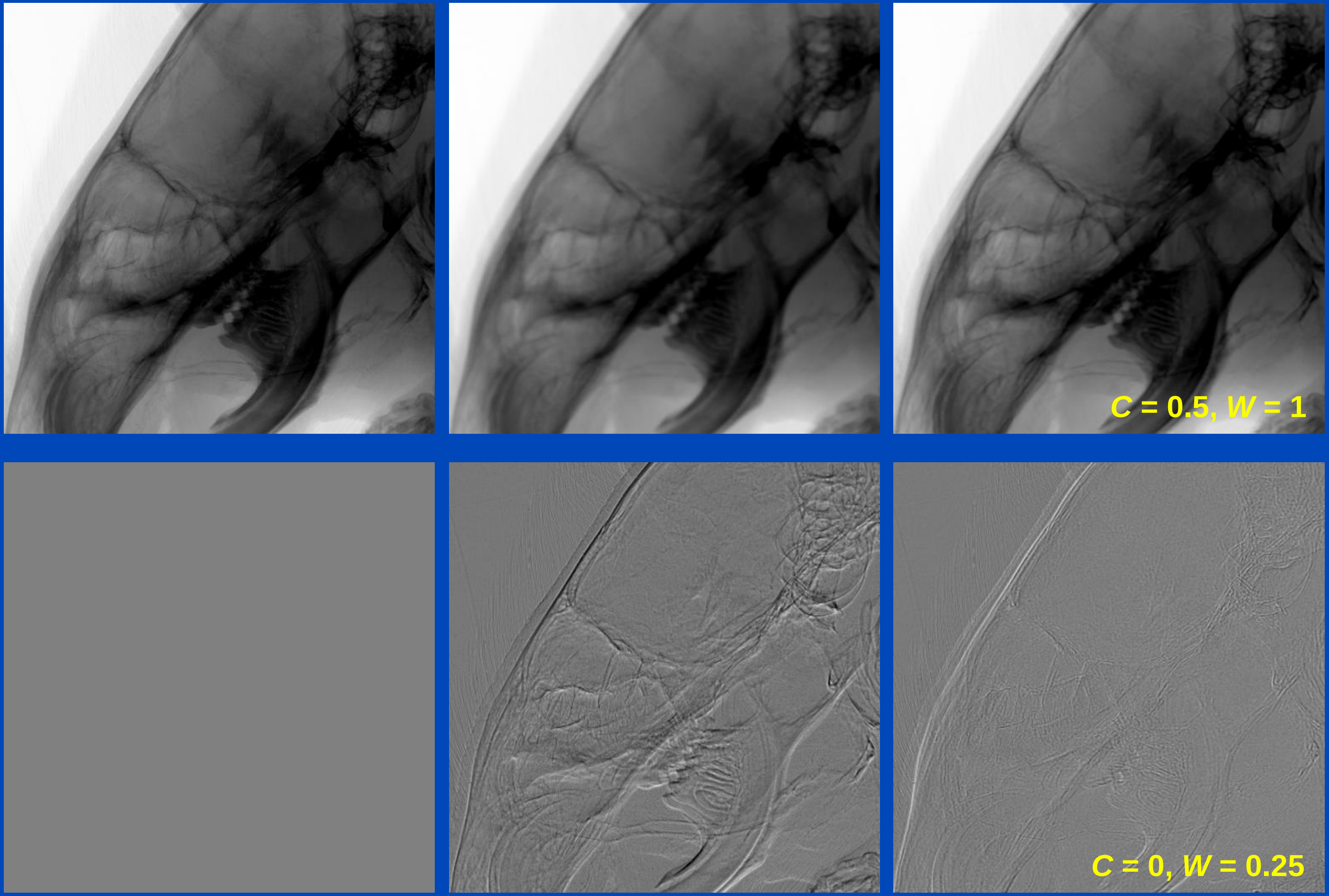

3D Simulations

- To evaluate the performance of the CNN deconvolution for 3D micro-CT imaging, the forward projection of several high resolution mouse datasets was used.
- The geometry of our experimental micro-CT system is
  - R_F = 80 mm
  - R_D = 500 mm

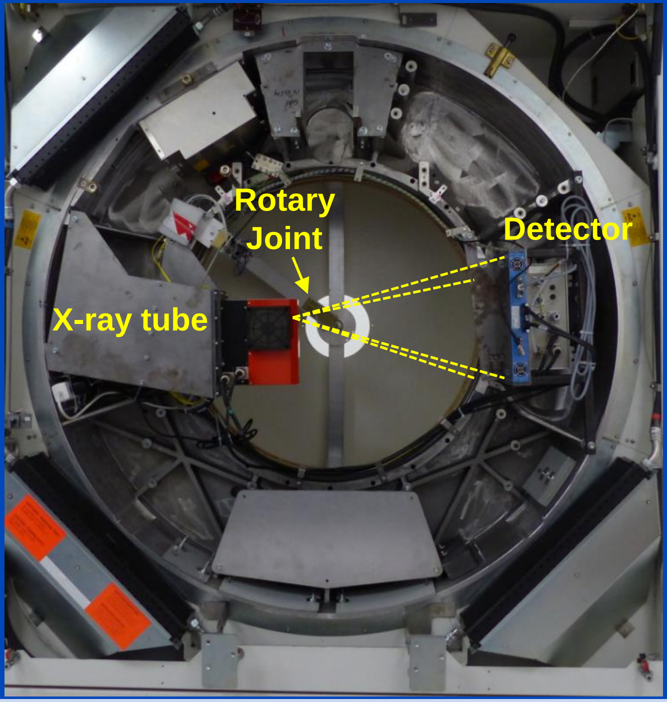

3D Simulations

- 1024 forward projections of one dataset were used for training over 100 epochs
- 1024 forward projections of another mouse dataset were used for testing
- Reconstructions of the deblurred projections were used to evaluate if the CNN deblurring introduces new artifacts into the reconstructed volume

3D Reconstructions of Simulated Projections

Reference image | **Blurred image** | **CNN deblurred image**

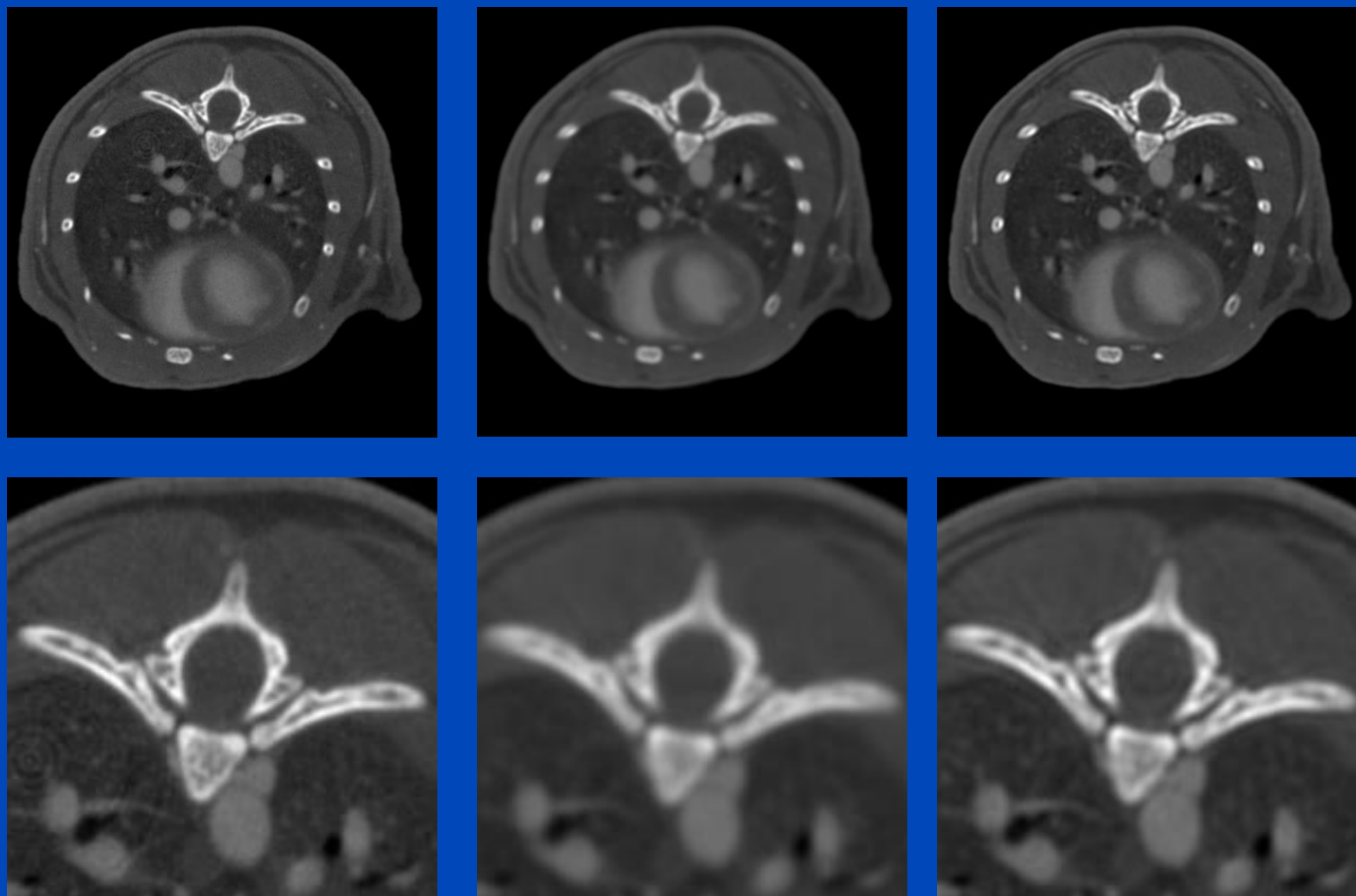

C = 2000 HU, W = 4000 HU

Discussion & Conclusion

- CNN deconvolution can be applied to x-ray projection images to increase spatial resolution
- CNN deconvolution performed better than RL reference method
- Our use case is to increase the tube power. Then CNN deblurring may help to reduce the measurement time.
- Training and application of the CNN can be performed without explicit knowledge of the system's PSF.
- Our results, however, are highly preliminary. A thorough performance analysis as well as an adjustment of the network structure and hyperparameters needs to be done.

Thank You!

This presentation will soon be available at www.dkfz.de/ct.
Job opportunities through DKFZ's international Fellowship programs (marc.kachelriess@dkfz.de).
Parts of the reconstruction software were provided by RayConStruct® GmbH, Nürnberg, Germany.
This work was supported in parts by the Deutsche Forschungsgemeinschaft (DFG) under grant SA 2776/1-1 and by the BMBF within the framework M2OLIE.